



HAL
open science

Role of hydrogen bonding in the capture and storage of ammonia in zeolites

I. Matito-Martos, A. Martin-Calvo, Conchi Maria Concepcion Ovin Ania, J.B. Parra, J.M. Vicent-Luna, S. Calero

► **To cite this version:**

I. Matito-Martos, A. Martin-Calvo, Conchi Maria Concepcion Ovin Ania, J.B. Parra, J.M. Vicent-Luna, et al.. Role of hydrogen bonding in the capture and storage of ammonia in zeolites. Chemical Engineering Journal, 2020, 387, pp.124062. 10.1016/j.cej.2020.124062 . hal-02746273

HAL Id: hal-02746273

<https://hal.science/hal-02746273>

Submitted on 6 Nov 2020

HAL is a multi-disciplinary open access archive for the deposit and dissemination of scientific research documents, whether they are published or not. The documents may come from teaching and research institutions in France or abroad, or from public or private research centers.

L'archive ouverte pluridisciplinaire **HAL**, est destinée au dépôt et à la diffusion de documents scientifiques de niveau recherche, publiés ou non, émanant des établissements d'enseignement et de recherche français ou étrangers, des laboratoires publics ou privés.

Matito-Martos I, Martin-Calvo A, Ania CO, Parra JB, Vicent-Luna JM, Calero S, Role of Hydrogen Bonding in the Capture and Storage of Ammonia in Zeolites, Chem. Eng. J 387 (2020) 124062.

10.1016/j.cej.2020.124062

hal-02746273v1

Role of Hydrogen Bonding in the Capture and Storage of Ammonia in Zeolites

I. Matito-Martos^a, A. Martin-Calvo^a, C. O. Ania^b, J. B. Parra^c, J.M. Vicent-Luna,^{a*} and S. Calero^{a*}

^aDepartment of Physical, Chemical, and Natural Systems, Universidad Pablo de Olavide. Ctra. Utrera km. 1. ES-41013 Seville, Spain

^bCEMHTI CNRS UPR3079, 45071, Orléans cedex 2, France

^cInstituto Nacional del Carbón, INCAR, CSIC, P.O. 73, 33080 Oviedo, Spain.

ABSTRACT

Ammonia is an important chemical compound used in a wide range of applications. This makes its capture, purification and recovery necessary. In this work we combine experimental and molecular simulation techniques to investigate the adsorption of ammonia using zeolites. Adsorption isotherms were measured in several commercial pure silica zeolites (including MFI, FAU, and LTA topologies), showing their potential to be used in large scale processes with lower cost than current techniques. In addition, we performed molecular simulations to describe the adsorption mechanisms from a microscopic point of view. We carried out Monte Carlo simulations to calculate the adsorption isotherms and to this aim we first developed a transferable set of potential parameters to describe the interactions of ammonia with the zeolites. We analyzed the adsorption energy between the adsorbents and the fluid involved in the adsorption

process and the effect of confinement on the microscopic structure of ammonia. This was compared with the liquid phase via radial distribution functions and hydrogen bond analyses. Here we describe the mechanisms that govern the adsorption of ammonia in zeolites as well as the effect exerted on the adsorption by the structural flexibility and by the presence of minimal amount of extra-framework species.

INTRODUCTION

The capture of ammonia is an important and challenging topic in industry and R&D due to the particular characteristics of this molecule. Ammonia is one of the most toxic, reactive, and corrosive gases used and produced at large scale in industrial processes. Annual production of ammonia can be measured in million metric tons, making it one of the most used chemicals.¹ The sustained exposition to high concentrations of ammonia could lead to severe health problems.²⁻⁵ The high toxicity of this chemical compound is perceptible even at low concentrations. Despite this, many applications involve the use of ammonia. This compound is largely used in agriculture as fertilizer, being one of the main source of ammonia emissions.⁶⁻⁹ It is also used to produce explosives, plastics, synthetic fibers and resins, and other numerous chemical compounds.^{10,11} Moreover, ammonia is employed in energy-related applications as working fluid in thermal batteries¹² or heat transfer processes¹³⁻¹⁵ and as fuel in internal combustion engines.¹⁶

Several technologies are used to mitigate the emissions of ammonia to the atmosphere, thus reducing the environmental impact. These solutions include membranes, biological and catalytic processes, and purification processes, among others.^{17,18} Adsorption processes have been proposed as a promising technique for the capture and storage of ammonia, and in this regard, nanoporous materials, such as metal organic frameworks (MOFs), zeolites, and activated carbons are used as adsorbents. Compared to activated carbons, MOFs and zeolites have shown higher affinity for ammonia. In the last years, MOFs have been largely studied for ammonia adsorption.^{11,15,16,18-20} However, despite the great adsorption capacities reported for MOFs, these materials suffer structural degradation after exposure to ammonia.^{15,19,20} Contrary to MOFs, zeolites exhibit greater stability towards ammonia adsorption,²¹⁻²⁵ making these materials an interesting alternative. Zeolites are composed by tetrahedral units formed by four oxygen atoms (O atoms) bonded to an atom of silicon, aluminum, or other metal (T atoms). In addition to

their stability, it is remarkable to note that zeolites entail lower production costs and a several commercial zeolites are available.

Due to the toxicity and reactivity of ammonia, there are not many studies of adsorption of this molecule in zeolites. Kazuo *et al.* investigated the acidic properties of mordenite zeolite with various Si/Al ratio by calorimetric measurements of the heat of adsorption of ammonia.²⁶ More recently Helminen *et al.* measured adsorption equilibrium isotherms of ammonia on 13X, 5A, 4A, and dealuminated faujasite zeolites showing interesting working capacities over a wide range of temperatures.^{27,28} In these works zeolites containing cations showed stronger ammonia adsorption than pure silica structures at low pressure^{27,28}. However, the hydrophobic nature of pure silica zeolites makes them better candidates in process involving humidity in order to avoid water competition.

The experimental investigation of ammonia capture is limited due to its hazardous nature. In this regard, molecular simulation is an excellent tool to gain insights on the adsorption mechanisms of ammonia, safe, and with low cost compared to experiments. Jaramillo *et al.* already explored the adsorption of ammonia in zeolite 4A using molecular simulation, providing a realistic force field that reproduces the adsorption in the zeolite.²⁹ Here, we study the ammonia adsorption capacity of several zeolites by combining experimental and computational techniques. We use pure silica zeolites with MFI, LTA, and FAU topologies. These structures differ in pore size and connectivity, which will be relevant on the analysis of the adsorption mechanism of ammonia. We measured adsorption isotherms of ammonia in the three structures at temperatures between 258 K and 298 K.

From the molecular simulation point of view there are not many studies of ammonia adsorption in zeolites, mainly due to the lack of force field parameters to describe the adsorbent-adsorbate interactions. Besides, the work of Jaramillo *et al.* focused in a zeolite 4A, where the interaction between ammonia and the extra-framework cations strongly affects the adsorption behavior.²⁹ In this work, we develop a transferable set of Lennard-Jones parameters to model the adsorption of ammonia in pure silica zeolites. We describe in detail the adsorption mechanism and the effect of confinement on the structure of ammonia within the pores of the zeolites. The structures are usually considered rigid, though sometimes they can exhibit structural flexibility. A structural phase transition of MFI zeolite induced by the fluid is discussed. Commonly, studies

refer to high silica zeolites as pure silica, which normally is an acceptable assumption. However, due to the reactivity of ammonia, a small amount of extra-framework cations could have a noticeable impact on the adsorption. For this reason, we also study the influence of the presence of cations. Finally, we compare the microscopic distribution of adsorbed ammonia with the distribution in the bulk.

METHODOLOGY

We calculated the adsorption isotherms using Monte Carlo simulations in the Grand Canonical ensemble (GCMC, i.e. μVT), where the average value of temperature (T), volume (V), and chemical potential (μ) are fixed. The chemical potential directly relates to fugacity, and fugacity to pressure by the fugacity coefficient, through the Peng-Robinson equation of state.³⁰ MC moves involve translation, rotation, reinsertion, and swap from the reservoir.³⁰ Provided adsorption points are collected after running 200.000 equilibration and 20.000 production cycles, respectively. Each cycle includes a number of MC cycles equal to the number of molecules in the system, with a minimum of 20 steps. The simulations are performed using the molecular simulation software RASPA.^{31,32}

Atomic interactions are modeled by electrostatic and van der Waals interactions. electrostatic interactions are taken into account with Coulombic potentials and using Ewald summations, while the van der Waals interactions are described by 12-6 Lennard-Jones potential.³⁰ The cutoff distance is set to 12 Å, where the interactions are truncated and shifted with no tail corrections applied and the periodic boundary conditions exerted in the three dimensions.³⁰ The described simulation conditions are commonly used to study adsorption in confined systems.^{33,34} The molecule of ammonia is modeled using TraPPE.³⁵ In this five-site model the repulsive and dispersive interactions are represented by a single LJ-site on top of the nitrogen atom. Additionally, three positive partial charges are set on top of the hydrogen atoms and a compensating negative charge is located at an extra dummy atom site (M). This site is placed on the C3 molecular axis and displaced 0.8 Å from the nitrogen atom towards the hydrogen atoms. Adsorbate-adsorbate van der Waals interactions are taken into account by Lorentz-Berthelot mixing rules.³⁶ To check the ability of the model of ammonia to reproduce its physicochemical properties, we calculated the vapor-liquid equilibrium (VLE) and the vapor pressure curves of the fluid. We obtain these

properties using MC simulations in the Gibbs ensemble.³⁰ In these simulations two boxes mimic two microscopic regions within the bulk phases away from the interface. During the simulation, temperature (T), total number of molecules (N), and system volume (V) remain constant. In order to fulfill the thermodynamic requirements for phase coexistence, each region should be in internal equilibrium and temperature, pressure, and chemical potential must be equal. These requirements are satisfied through a variety of MC moves including displacement of particles within and between the regions and volume fluctuations boxes. **Figure S1** in the ESI compares the VLE and saturation vapor pressure of ammonia with experimental data taken from NIST.³⁷ We found excellent agreement between calculated and experimental values of the VLE. This indicates that the model can reproduce the temperature dependence on the density of ammonia in the liquid and gas phases at saturation pressure. The saturation pressure is also calculated and compared to the experimental values and to the value predicted by the Peng-Robinson Equation of State (PREoS). The prediction of the saturation pressure from PREoS agrees with experiments and can be used to relate chemical potential and fugacity in Grand-Canonical simulations.

The adsorbate-framework Lennard-Jones interactions are defined by the oxygen atoms of the framework (O_{zeo}) with the atoms of the adsorbed molecules. The set of charges for the framework atoms has been taken from Garcia-Sanchez *et al.*,³⁸ while the adsorbate-framework Lennard-Jones parameters have been independently fitted in this work to experimental adsorption data.

From the experimental side, the high silica zeolite with faujasite topology CBV901 (ratio Si/Al = 40) was obtained from Zeolyst International, while pure silica MFI and ITQ-29 (zeolite with LTA topology) were kindly supplied by ITQ (CSIC). Simulations were carried out using the pure-silica version of these zeolites as well as the aluminosilicate version of FAU with five extra-framework protons (H^+) covering the experimental Si/Al ratio = 40. To do so, we generated 50 structures with the aluminum/silicium substitutions in different positions and obeying the Lowenstein rule, keeping the most stable (energetically). To take into account the interaction of ammonia with the protons, we exchanged them by ammonium cations (NH_4^+). Protons are modeled by a single point charge which compensates the negative charge of the structure resulting from the Si/Al substitutions to reproduce the experimental ratio. The Lennard-Jones parameters for the ammonium cations are taken from Jorgensen *et al.*,³⁹ while the charges have been rescaled (**Table 1**) according to the set of charges for the

framework atoms.³⁸ During MC simulations, all frameworks have been considered rigid as it is known that the effect of the zeolite flexibility is usually minor on the adsorption of small molecules at the temperatures under study.⁴⁰ However, we carried out energy minimization simulations to optimize the structures according to their most stable configuration. These simulations were performed by using the Baker's method⁴¹ and the core-shell potential of Sanders *et al.*^{42,43} which has demonstrated high accuracy for the structural zeolite description.^{44,45} Structural properties such as surface area (SSA), void fraction, and pore volume (PV) were also calculated for further analysis and to compare with experimental results. SSA was obtained by rolling a helium molecule over the surface of the zeolite to estimate the amount of overlap with other framework atoms. The SSA was obtained by multiplying the fraction of overlap by the area of the probe molecule over all framework atoms. The void fraction was measured using helium at room temperature and the Widom test particle insertion method.⁴⁶ The pore volume (PV) was calculated from the void fractions, multiplying by the volume of the unit cell. Additional information about these methods can be found elsewhere.³⁰ The textural features (surface area and pore volume) were also experimentally calculated from high resolution nitrogen adsorption isotherms at 77 K, recorded in a volumetric analyzer (ASAP 2020, Micromeritics) provided with a turbomolecular vacuum pump and three pressure transducers for accuracy in the low pressure region. The zeolites were previously outgassed at 623 K (1 K min⁻¹) overnight.

Figure 1 and S2 in the ESI show a representation of the pore space and the calculated pore size distributions (PSD) of the selected zeolites, respectively. The PSD is calculated geometrically by using the method of Gelb and Gubbins.^{47,48} Additional structural properties obtained from simulations and experiments are summarized in **Table 2**. The structure of MFI exhibits a phase transition depending on temperature and/or loading.⁴⁹⁻⁵¹ At values of temperature higher than 300 K MFI shows an orthorhombic structure with space group *Pnma*; while at lower values of temperature, it exhibits a monoclinic structure with space group *P21/n.1.1*. Here we use the crystallographic positions of the MFI zeolite taken from van Koningsveld *et al.* for the orthorhombic⁵² and monoclinic⁵³ structures. In both cases, the topology of this zeolite consists of main straight channels limited by 10-membered (10MR) rings windows (*x*-axis), intersected by zig-zag secondary channels leading to a 3-dimensional system with limiting diameters of about 4.5 - 4.7 Å. These two systems of channels can be seen in the PSD from **Figure S2** (peaks at ca. 6 and 5 Å respectively). Calculated surface area

and pore volume for MFI are in good agreement with experiments as can be observed in **Table 2**. ITQ-29 and FAU, have cubic cells of 11.87 and 24.26 Å, respectively. We used the crystallographic positions reported by Corma *et al.* (ITQ-29),⁵⁴ and Hriljac *et al.* (FAU).⁵⁵ ITQ-29 and FAU show two types of interconnected cages (as can be seen from the two main peaks in the PSD in **Figure S2**). In FAU, big cages (α -cages) are accessible through 12MR windows, with a limiting diameter of around 7.1 Å; while in ITQ-29, LTA-cages are accessible through an 8MR window, resulting on a lower limiting diameter (4.1 Å). β -cages or sodalities, from the two structures, are not accessible for most molecules due to the narrow windows that connect them with the α -cages (4- and 6-membered-rings, respectively). However, the small size of ammonia allows this molecule to enter in the sodalities cages. Regarding the surface area, experimental and simulated values for ITQ-29 are in agreement, with less than 10% of discrepancy. However, in the case of FAU, Martin-Calvo *et al.*⁵⁶ already found that the zeolite used in the experimental measurements (CBV901) has a surface area of c.a. 700 m²·g⁻¹, while the structure used for simulations has a surface area of c.a. 1000 m²·g⁻¹. This difference is responsible of variations on the saturation capacity of about 20%. However, using a correction factor of 0.79 in the calculated adsorption values, experimental and simulated isotherms match.

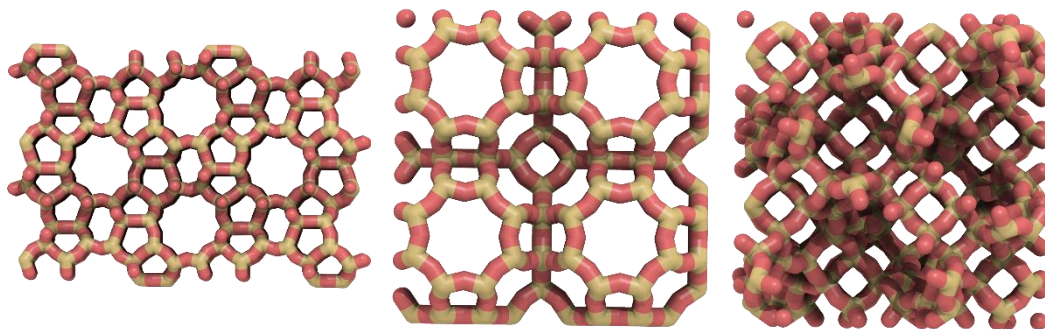


Figure 1. Representative structure of (from left to right) MFI, ITQ-29 and FAU. Oxygen and silicon atoms are depicted in red and yellow, respectively.

Table 1. Lennard-Jones parameters and point charges of the adsorbates and the zeolite.

Atom 1	Atom 2	ϵ/k_B (K)	σ (Å)	Charge (e ⁻)
Adsorbed Molecules / Extra framework cations				
N(NH ₃)	N(NH ₃)	185.000	3.420	0.000
H(NH ₃)	H(NH ₃)	-	-	0.410

Dum(NH ₃)	Dum(NH ₃)	-	-	-1.230
N(NH ₄)	N(NH ₄)	85.637	3.250	-0.154
H(NH ₄)	H(NH ₄)	-	-	0.134
Zeolite				
O(zeo)	O(zeo)	-	-	-0.393
Si(zeo)	Si(zeo)	-	-	0.786
Oa(zeo)	O(zeo)	-	-	-0.414
Al(zeo)	Al(zeo)	-	-	0.486
Zeolite - Adsorbed Molecules / Extra framework cations				
N(NH ₃)	O(zeo) / Oa(zeo)	160.000	3.125	-
H(NH ₃)	O(zeo) / Oa(zeo)	-	-	-
Dum(NH ₃)	O(zeo) / Oa(zeo)	-	-	-
N(NH ₄)	O(zeo) / Oa(zeo)	85.637	3.270	-
H(NH ₄)	O(zeo) / Oa(zeo)	-	-	-

Table 2. Structural properties of the zeolites.

Zeolite	Si/Al ratio	Surface area m ² g ⁻¹	Pore Volume cm ³ g ⁻¹
<i>Simulations</i>			
MFI (orthorhombic)	∞	548	0.160
MFI (monoclinic)	∞	548	0.151
ITQ-29	∞	947	0.327
FAU(SI)	∞	1088	0.360
FAU(NH₄⁺)	40/1	1009	0.344
<i>Experimental</i>			
MFI	∞	383/491*	0.180
ITQ-29	∞	802	0.330
CBV-901 (FAU)	40/1	706	0.300

*The SSA values correspond to the calculations before and after the phase transition in the N₂ adsorption isotherm.

In addition to MC simulations, we performed molecular dynamics (MD) to obtain the structural-related properties of ammonia in the liquid phase. The simulation box consists of a cubic box of 25 Å of side length containing 360 molecules of ammonia randomly placed by MC insertions. The starting system size is fixed to the experimental density of liquid ammonia at 273 K and 1 bar (652 kg/m³).³⁷ We performed a first equilibration MD simulation in the NPT ensemble to relax the system in its equilibrium volume followed by a production run in the NVT ensemble.

The experimental adsorption isotherms of ammonia on the studied zeolites were carried out in a volumetric analyzer (ASAP 2010, Micromeritics) at temperatures near ambient conditions (ca. 258-298 K); the samples were previously outgassed at 623 K for 6

hours. The temperature was controlled using a thermostatic circulating oil bath. High purity ammonia (i.e., 99.95%) was supplied by Air Products.

RESULTS AND DISCUSSION

Zeolites not always obey generic mixing rules and in these cases, the interaction Lennard-Jones parameters with the gases need to be independently adjusted.^{38,57} Here we obtain the parameters that describe ammonia-zeolite interactions by fitting the simulation results to the experimental adsorption isotherm of ammonia in MFI zeolite at 288 K. We further validate the parameters for three additional temperatures spanning from 258 K to 288 K. In addition, we confirmed the transferability of the force field parameters to other zeolites, such as ITQ-29 and FAU.

Figure 2 shows the calculated and experimental adsorption isotherms of ammonia in monoclinic MFI,⁵³ while the fitted parameters are compiled in **Table 1**. The figure shows an excellent agreement between calculated and experimental isotherms at the highest values of temperature (288 K and 273 K) for the full range of pressure. The agreement for the other values of temperature (258 K and 263 K) is also reasonably good up to medium-high coverage (around 3 mol·kg⁻¹). However, at certain pressure (c.a. 25-50 kPa, depending on temperature), the experimental isotherms exhibit a sudden increase in the uptake. Such unusual effect is not observed in the calculated isotherms at low temperatures (e.g. 258 and 263 K); nevertheless, the agreement between the experimental and calculated isotherms at high temperature is excellent. This behavior suggests that a phase transition occurs during the adsorption of ammonia, as already reported for MFI zeolite for nitrogen and argon adsorption at cryogenic temperatures.⁵⁸⁻⁶⁰

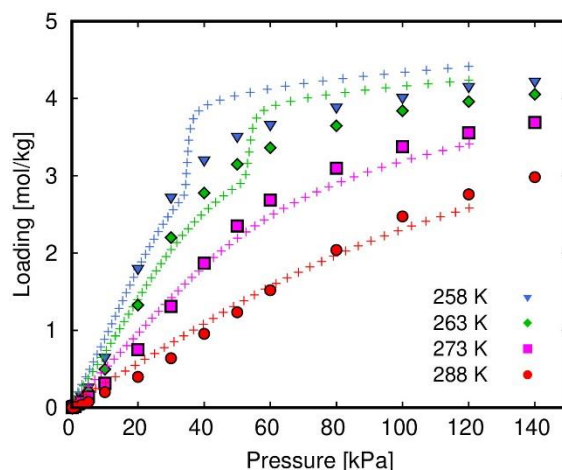


Figure 2. Calculated (closed symbols) and experimental (crosses) excess adsorption isotherms of ammonia in monoclinic MFI at temperatures between 258 K and 288 K.

The adsorbent and the adsorbate could endure phase transitions that would explain the experimental observations. Ammonia liquefaction inside the pores of the zeolite is possible as a consequence of confinement. However, attending to the shape of the experimental isotherm, this is not likely. In such case, one would expect the sharp rise of the uptake at lower values of pressure. Another explanation could be the structural phase transition of MFI upon ammonia adsorption, as already reported for other small probes (e.g., nitrogen, argon at cryogenic temperatures).⁵⁸⁻⁶⁰

Figure 3 shows the adsorption isotherms of ammonia in MFI at the lowest and the highest temperatures studied (i.e., 258 K and 288 K, respectively) in the monoclinic and orthorhombic structures. The simulated isotherms for the monoclinic structure are in good agreement with experimental ones at 288 K and in the low-pressure regime of the isotherm at 258 K (up to 30 kPa). Interestingly, for the orthorhombic structure, the calculated isotherms are closer to the experimental values at pressures above 30 kPa (well beyond the Henry regime). This is an indication that the monoclinic form of MFI changes to orthorhombic upon adsorption of ammonia. As can be seen in **Figure 2**, the step on the adsorption isotherms appears at different pressures for 258 and 263 K, but at a similar loading, i.e. 2.8-2.9 mol/kg. On the other hand, the adsorption isotherms at 273 and 288 K do not show this effect. This could be attributed to i) the fact that the loading at these temperatures barely reaches the threshold of 2.8-2.9 mol/kg mentioned above, and/or ii) the increased mobility of the adsorbate at higher temperatures, that would

decrease its density, thus reducing the interaction of ammonia with the walls of the zeolite. For this reason, the effect is only observed at low temperature, where the pressure induced by the confined adsorbate is higher. Unfortunately, such phase transition is a rare event that cannot be observed by classical simulations, since an accurate description of the adsorption processes in flexible structures is still challenging.

Previous studies about the phase transition of MFI have been reported in literature. Grau-Crespo *et al.*⁶¹ studied the monoclinic to orthorhombic phase transition of the empty MFI against temperature using a free energy minimization method. In this work, we have performed energy minimization simulations at 0 K to relax the structures to their most stable configuration. We used the NPTPR ensemble where all the cell lengths and angles are allowed to vary independently. We did not find any structural change when the energy minimization calculation starts from the monoclinic structure. However, starting from the orthorhombic structure we obtained the monoclinic form. **Figure S3** in the ESI shows the results of the adsorption isotherms calculated in the optimized structure (resulting from the geometric optimization of the orthorhombic structure) at 258 K, which are very similar to the results obtained in the original monoclinic MFI. We have proved that the orthorhombic to monoclinic phase transition is easy to reproduce by performing energy minimization simulations in absence of temperature. Several causes for the inverse phase transition, i.e. monoclinic to orthorhombic have been reported in literature. These causes are usually variations of temperature or pressure^{61,62} and T atoms substitution by trivalent or tetravalent elements⁶³. In this work, we show that adsorbed ammonia could also induce the phase transition.

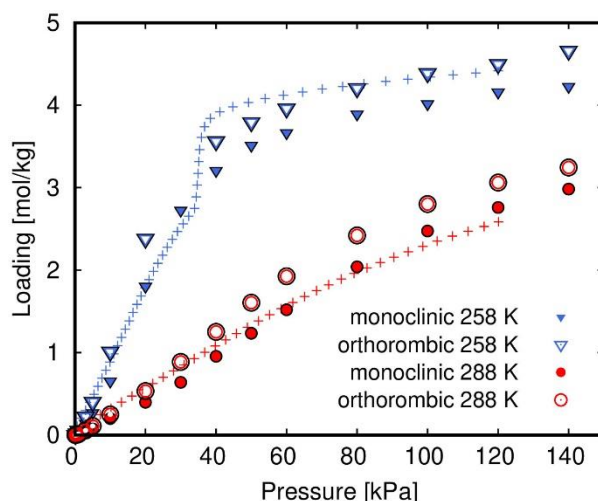


Figure 3. Calculated and experimental (crosses) excess adsorption isotherms of ammonia in monoclinic MFI (closed symbols) and orthorhombic MFI (open symbols) at 258 K and 288 K.

To check the transferability of the developed ammonia-zeolite interaction parameters, we compared the adsorption isotherm of ammonia in other topologies at several temperatures. **Figure 4** shows the comparison for ITQ-29 zeolite, the pure silica version of LTA zeolite. Despite a slight underestimation of the loading in the low-pressure range, there is a good agreement between the experimental and calculated values. These differences on adsorption can be attributed to small imperfections of the zeolites particles, which could act as adsorption sites favoring the adsorption of the first molecules entering the structures. The crystals used for the simulations are ideal, which would explain the higher starting pressure needed for the molecules to be adsorbed. However, the saturation capacity and the shape of the curves are well reproduced. In ITQ-29, the increase in the amount adsorbed at high relative pressures is not attributed to a phase transition, but rather to a nucleation of the fluid inside the big cavities of this zeolite. This fact will be discussed in detail later.

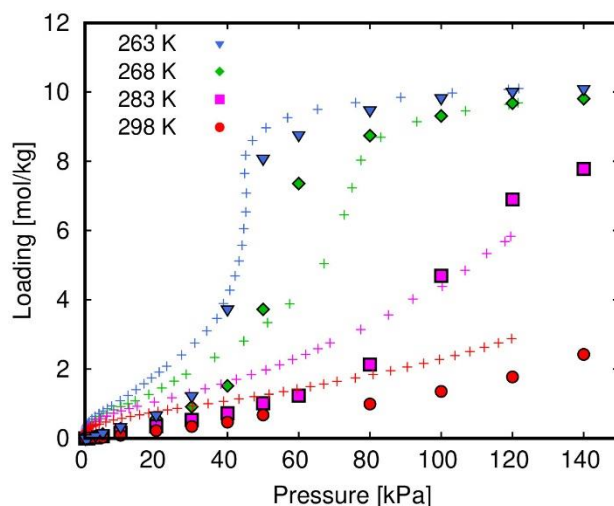


Figure 4. Calculated (closed symbols) and experimental (crosses) excess adsorption isotherms of ammonia in ITQ-29 at temperatures between 263 K and 298 K.

The last zeolite under study is the commercial zeolite CBV-901 or high-silica FAU. **Figure 5** shows the calculated and experimental adsorption isotherms of ammonia in FAU at 258 and 263 K. We found discrepancies between experiments and simulations, which can be explained by two independent effects. As seen, both the experimental and calculated adsorption isotherms show an abrupt step at pressures between 40 and 60 kPa. The step of the calculated adsorption isotherms takes place at higher pressures than on the experiments. In addition, the experimental loading is underestimated in the calculated isotherms before the adsorption step and overestimated after that. As previously reported,⁵⁶ the overestimation of the saturation loading is due to the large difference between the measured and calculated specific surface areas of zeolite CBV-901 used in the experimental assays, and pure silica FAU zeolite used in the simulation (see **Table 1**). The proposed correction factor of 0.79 only solves the discrepancies on the adsorption of ammonia at high pressure, while the underestimation of the loading in the low coverage regime is still not explained. To account for this behavior we must bear in mind that CVB-901 is a high-silica zeolite with a Si/Al ratio of 40, which means that it contains a low (but non negligible) amount of extra-framework protons.⁶⁴ This modifies slightly the electrostatic field inside the pores of the zeolite. This fact does not affect the adsorption of small gases or other non-polar molecules. However, ammonia is a very reactive compound that could interact strongly with impurities or extra-framework cations present in the zeolite. To further verify this hypothesis, we performed GCMC simulations for ammonia in the FAU structure containing five Al

atoms and five protons. Ammonia molecules react with protons providing ammonium cations (NH_4^+), where the new covalent bond created is indistinguishable from the other N-H bonds. Unraveling the mechanism of this reaction is out of the scope of this work; however, a simplification can be done to study the effect of the possible ammonium cations formed during the adsorption process. We started the simulation with the structure loaded with five ammonium extra-framework cations, assuming that five protons react with five molecules of ammonia. These five molecules of ammonia (0.43 mol/kg) will be added to the total adsorption loading at the end of the simulation, though it has not significant effect on the adsorption. **Figure 5** (bottom) shows the effect of having five protons or five ammonium extra-framework cations on the adsorption of ammonia at 258 K in FAU zeolite. The experimental adsorption isotherm can be better reproduced by the addition of either of them (and applying the 0.79 correction factor to the entire isotherm). As seen, the effect of the low number of cations is crucial in the low-pressure range which now agrees perfectly with the experimental data. The presence of cations also lowers the pressure at which the step appears in the calculated isotherms; however, it has a negligible effect on the saturation loading.

Based on the discussed results, we can confirm that the developed Lennard-Jones parameters for the interaction between ammonia and pure silica MFI zeolite are transferable to different topologies. However, unusual phenomena associated to adsorbate induced flexibility, or its interaction with low concentrations of impurities or extra-framework species should be carefully studied for an accurate description of the adsorption process.

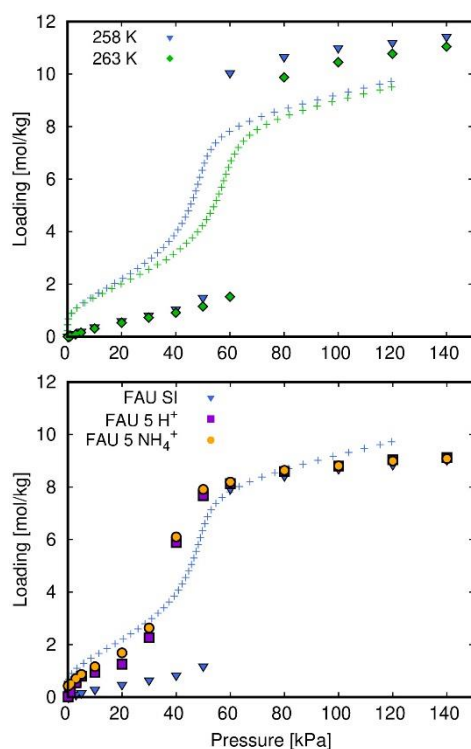


Figure 5. Calculated (closed symbols) and experimental (crosses) excess adsorption isotherms of ammonia in FAU (CBV-901) at temperatures between 258 and 263 K. The figure on the top contains simulation results for the pure silica version of FAU, while the figure on the bottom contains the results for the aluminosilicate FAU with 5 protons or 5 ammonium cations at 258 K. The values of this last figure are rescaled by a factor of 0.79 according to the work of Martín-Calvo *et al.*⁵⁶

For applications related to capture of ammonia, zeolites showing high capacity are desirable. In addition to high capacity, it is convenient to choose zeolites with stepped adsorption isotherms. Common processes used in industry are pressure or temperature swing adsorption, therefore a stepped isotherm minimizes the temperature or the pressure lift when adsorption and desorption takes place, hence reducing the cost of the process. Taking this into account, we compared the adsorption isotherms of ammonia in the three selected zeolites (see **Figure 6**). As expected based on their differences in pore volume and surface area (**Table 2**), MFI exhibits the lowest adsorption capacity (about 4 mol/kg) compared to ITQ-29 and FAU (about 10-12 mol/kg). Moreover, ITQ-29 and FAU show stepped isotherms at 263 K that indicate the possible release of the 80% of the adsorbed ammonia by variations of pressure from 60 to 20 kPa. This fact, together with their relatively high capacity, stability, and commercial availability make these zeolites interesting candidates for the capture of ammonia by pressure swing adsorption

processes. Similar yields can be achieved in a temperature swing adsorption process, with a working pressure of about 1 bar and varying the temperature from 263 to 298 K. Usually, materials with large cavities adsorb light molecules at very high pressures compared to materials having smaller cavities.

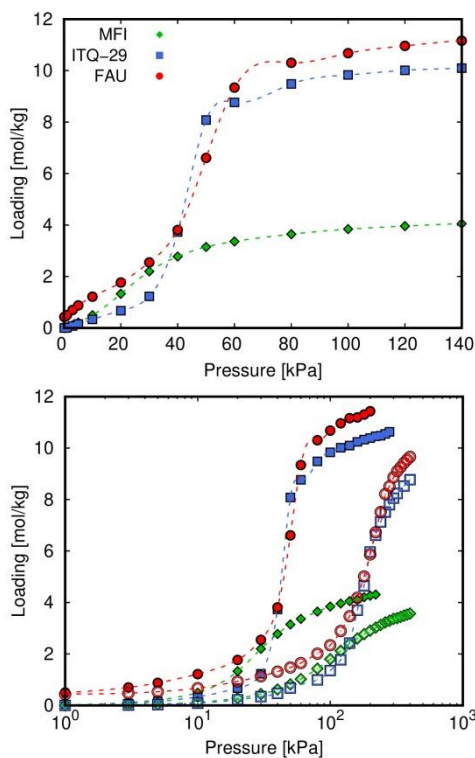


Figure 6. Excess adsorption isotherms of ammonia in MFI, ITQ-29, and FAU zeolites at 263 K (top) and at 263 K (closed symbols) and 298 K (open symbols) in logarithmic scale (bottom). Dashed lines are eye guidelines.

For energy-related applications such as heat transfer and heat pump devices where ammonia acts as refrigerant, a stepped adsorption is also desirable. Using adsorption/desorption cycles in a thermal energy storage process, energy can be produced and stored due to the exothermic nature of the adsorption process. The adsorption energy involved in the adsorption process is a key factor. **Figure 7** shows the absolute value of the isosteric heat of adsorption as a function of the adsorbed amount of ammonia in the three zeolites. The general trend shows an increase in the heat of adsorption when the loading of ammonia increases. MFI shows a linear trend from 20 kJ/mol at low coverage to 35 kJ/mol at saturation. ITQ-29 and FAU show similar

trends, with a small decrease in the heat of adsorption at low coverage, followed by an increase from about 20 kJ/mol up to 35-40 kJ/mol at saturation conditions.

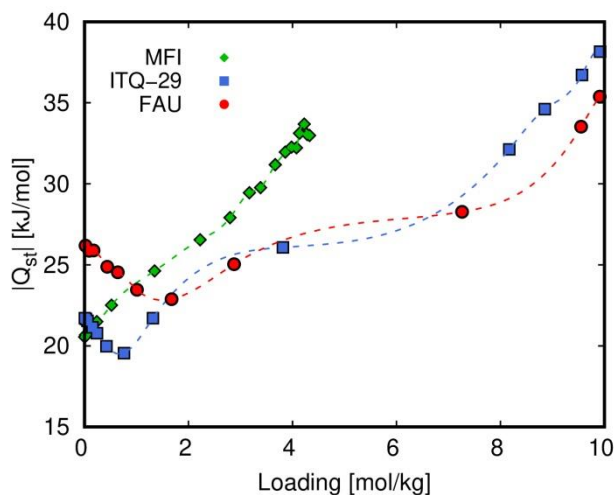


Figure 7. Absolute value of the isosteric heat of adsorption as a function of the loading of ammonia in MFI, ITQ-29, and FAU. Dashed lines are eye guidelines.

The isosteric heat of adsorption is a magnitude that takes into account the strength of the interaction between the fluid and the adsorbent on adsorption processes. To study in detail the origin of these values of energy we analyzed the contribution of the internal energy to the heat of adsorption. Since the structures are modeled as rigid crystals, the potential energy involved in the process comes from the fluid-adsorbent and fluid-fluid interactions. **Figure 8** shows the absolute value of the zeolite-ammonia and ammonia-ammonia potential energy divided by the number of molecules of adsorbed ammonia. As for the isotherms, ITQ-29 and FAU behave similarly, while differences are observed on MFI. The MFI-ammonia potential energy is almost constant for the entire pressure range. ITQ-29-ammonia and FAU-ammonia energies show two clear linear regimes with a reduction of 7-8 kJ/mol below 50 kPa. This pressure corresponds to the step of the adsorption isotherms. Close to saturation pressure, the zeolite-ammonia potential energy is constant and about 13 kJ/mol. The ammonia-ammonia energy agrees with the behavior found for the adsorption isotherm. The values of potential energy are almost twice for ITQ-29 and FAU than for MFI at saturation conditions, and they show the same step. This is an indication that the interplay between molecules of ammonia governs the adsorption process. In fact, the adsorption of ammonia in zeolites with large cavities is governed by the nucleation of these molecules. This is not very surprising

since ammonia can form a hydrogen bond network similar to that found for water or light alcohols. A high nucleation level of ammonia implies a high energetic exchange, which can be used efficiently for energy-related applications. This nucleation depends on the topology of the zeolite, being more important for zeolites with large cavities such as ITQ-29 and FAU (see **Figure 1 and S2** in the ESI).

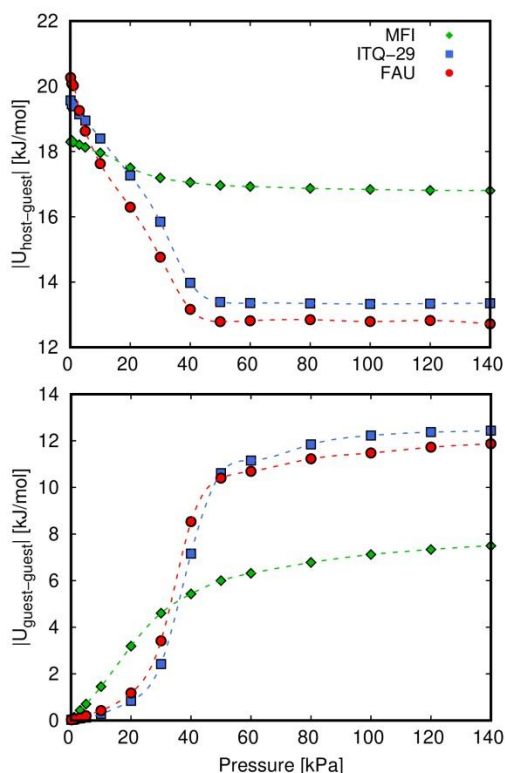


Figure 8. Absolute value of zeolite-ammonia (top) and ammonia-ammonia (bottom) interaction energy per adsorbed molecule at 263 K. Dashed lines are eye guidelines.

To gain insights into the nucleation process of ammonia within the pores of the zeolites, we analyzed the hydrogen bond formation among the adsorbed molecules. To this aim, we used a geometric criterion to estimate if two close molecules are bonded via a hydrogen bond. This criterion is related with the behavior of the RDFs between the ammonia atoms. **Figure 9** shows the N-N, N-H, and H-H RDFs corresponding to ammonia confined in the cavities of the three zeolites at saturation conditions at 263 K. We compared the results with the RDFs from MD simulations of ammonia in the bulk and the experimental data reported by Ricci *et al.*⁶⁵ We observed a good agreement between the experimental RDFs and the calculated RDFs in the bulk, corroborating once more the accuracy of the model selected for ammonia. It is worth noting that

experimental N-H and H-H RDFs show a series of first peaks not shown in the calculated RDFs. These peaks stand for the intramolecular N-H and H-H distances, while we discard the intramolecular distances. The behavior of confined ammonia is similar to this in the bulk, where the first peaks are in the same position but shifted to higher intensities. This indicates that the microscopic organization of confined ammonia is the same than in the bulk. The increase in the intensity of the peaks can be explained by the fact that in the bulk, one molecule is surrounded by other molecules in all directions, however in confinement, molecules close to the zeolite walls are surrounded by other molecules only in the opposite direction to the walls. This is taken into account in the RDF normalizing by the number of molecules into the coordination shell. According to these RDFs we can extract information related to the hydrogen bonds involved in the adsorption process.

We used two criteria to estimate the existence of the hydrogen bond: i) if the N-H intermolecular distance is lower than 2.7 Å and ii) if the N-N distance is lower than 5 Å. These distances are based on the respective RDFs and a previous work from the literature. Boese *et al.*⁶⁶ reported a study of the liquid phase of ammonia with ab initio calculations. They used the same criterion that we are using, with a N-N cut off of 5.1 or 5.5 Å depending on the functional used, but accordingly to the first minimum of the N-N RDF. They reported that the N-H cut off distance cannot be determined in the same way, since there is no clear minimum that separates the hydrogen-bonded and non-bonded H atoms in the N-H RDF. However, the N-H RDF shows a shoulder in the first peak which is associated to the hydrogen-bonded H atoms. This shoulder merges into the broad and more intense peak corresponding to the non-bonded H atoms of the first solvation shell. They identified that this shoulder extends up to 2.7 Å and used this value as N-H cut off distance. Moreover, He *et al.*⁶⁷ studied the hydrogen bond network of liquid ammonia via MD simulations using a polarizable force field. They stated that the hydrogen bond formation is recognizable in N-H distances around 2.7 Å too. From an experimental point of view, Ricci *et al.*⁶⁵ studied the microscopic structure of liquid ammonia at low temperatures by neutron diffraction experiments. They agree with the other authors that hydrogen bonds in ammonia are related to N-H intermolecular distances lower than 2.7 Å. Using this criterion and confirming that the microscopic organization of ammonia is conserved in confinement, we estimated the average number of hydrogen bonds per ammonia molecule (nHB) in the cavities of the zeolites.

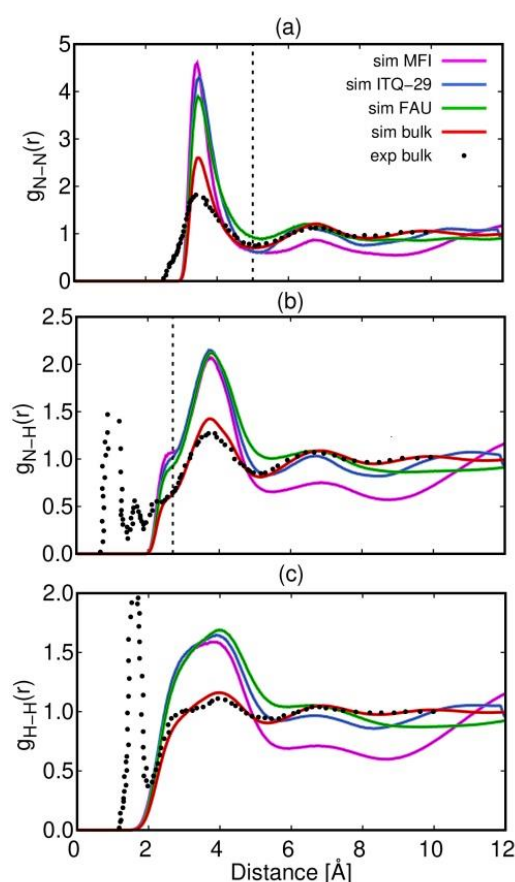


Figure 9. Radial distribution functions of nitrogen-nitrogen (a), nitrogen-hydrogen (b), and hydrogen-hydrogen (c) from MC simulations at 263 K in the three zeolites. The radial distribution functions in bulk taken from MD simulations and taken from experiments reported by Ricci *et al.*⁶⁵ at 273 K are also included for comparison. Vertical dotted lines in (a) and (b) represent the cut off value considered for the calculation of hydrogen bonds.

Figure 10 shows the nHB of confined ammonia as a function of pressure. We compare with the data obtained in the bulk by MD simulations and the value reported by He *et al.*⁶⁷. The nHB obtained from the simulation in the bulk are in excellent agreement with these obtained by He *et al.*⁶⁷ via MD simulations based on a polarizable force field and with experimental and computational results for the study of liquid ammonia found in the literature.^{65,66,68} In the case of confined ammonia, we observed a behavior similar to the adsorption isotherms or ammonia-ammonia values of potential energy. This confirms that the adsorption of ammonia in pure silica zeolites is governed by the nucleation of this molecule inside the cavities. At saturation, ITQ-29 and FAU show that the nHB of confined ammonia is about 1.2, while the value in the bulk is about 1.6-

1.7. This indicates that confinement slightly weakens the hydrogen bond network of ammonia, but it is still strong inside the large cavities of these zeolites. However, the nHB considerably decreases inside the interconnected channels of MFI up to a value of 0.6 at saturation. **Figure S4** shows the average occupation profiles of ammonia inside the cavities of the three zeolites at low, medium and high coverage from simulations corresponding to the lowest temperature (i.e. 258 K for MFI and FAU and 263 K for ITQ-29). The average occupation profiles represent the most probable positions of finding adsorbate molecules within the pores of the structures. The representation of the average occupation profiles is the projection over a given plane of the center of mass coordinates of the molecules. The positions of the atoms are recorded during the whole simulation and averaged over 10^3 configurations. **Figure S4** shows that the ammonia molecules form clusters in the large cavities of ITQ-29 and FAU, and at the intersections of MFI. The most probable binding sites of ammonia in ITQ-29 and FAU are the planes formed by the rings at the big cavities. These binding sites allow the nucleation of the fluid in the cages for increasing pressure via the formation of hydrogen bond network. **Figure 11** shows an example of this hydrogen bond network. The figure contains representative snapshots of ammonia molecules forming hydrogen bonds in the bulk and confined in the three zeolites. Ammonia in ITQ-29 and FAU is organized in three dimensions, similarly than in the bulk. The narrow channels of MFI only allow forming hydrogen bonds in a linear network along the interconnected two-dimensional channels system.

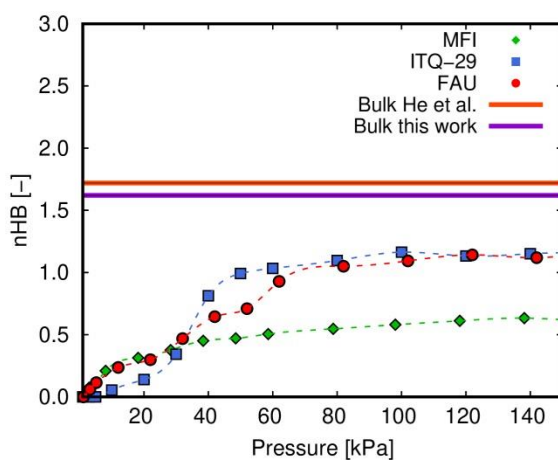


Figure 10. Average number of hydrogen bonds per molecule as a function of the pressure taken from simulations at 263 K. The value of the average number of hydrogen bond in bulk phase

taken from MD simulations and reported by He *et al.*⁶⁷ at 273 K is added for comparison. Dashed lines are eye guidelines.

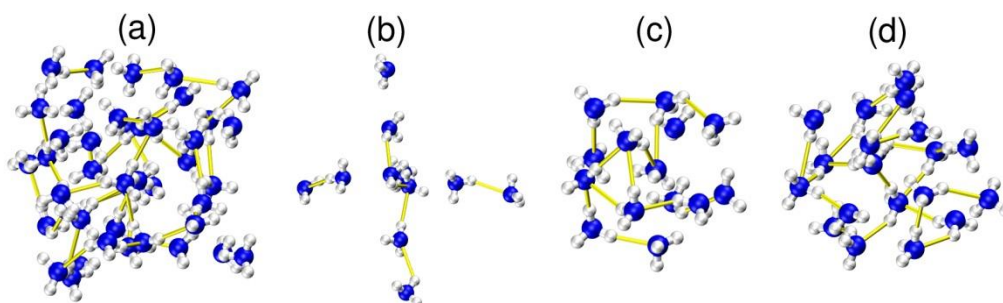


Figure 11. Representative snapshot of the molecules of ammonia bonded via hydrogen bonds in a cubic region of the bulk of 10 Å side length (a), and confined in MFI (b), ITQ-29 (c), and FAU (d).

The structural information obtained from the analysis of the RDFs, the nHB, and the average occupation profiles explain the behavior of the adsorption process. The trends of the adsorption isotherms are linked to the nucleation of the adsorbates by the formation of hydrogen bonds. In this regard, the process of the formation of hydrogen bonds with increasing pressure entails an energetic exchange confirmed by the study of the heats of adsorption and the interaction energies. The results of this work show the connections between the microscopic structure of the fluid, the energy involved, and the adsorption of ammonia in pure silica zeolites.

CONCLUSIONS

We combined classical molecular simulations with experimental techniques to study the adsorption of ammonia in three commercial zeolites namely MFI, ITQ-29, and FAU. We validated the model of ammonia by reproducing characteristic properties of the adsorbate in the liquid and the vapor phase, such as the VLE or the saturation pressure, and the microscopic structure of ammonia liquid based on hydrogen bonds and RDFs. Using this model, we developed a transferable set of parameters for the interactions of ammonia with the zeolite that describes in detail the adsorption in pure silica adsorbents. The model is validated by comparison with experiments in the three zeolites at values of temperature ranging from 258 to 298 K. We also demonstrated that contrary

to other small gases or non-polar molecules, the adsorption of ammonia could be influenced by distinct factors that should be analyzed in detail: a) the induced flexibility of MFI, which suffers a structural phase transition from the monoclinic to an orthorhombic structure, and b) the presence of small concentration of impurities such as extra-framework protons or ammonium cations, is a determining factor to reproduce the experimental measurements. The energetic and structural analysis of ammonia during adsorption confirm that the adsorption process is governed by the nucleation of the fluid. Based on the results of this work, it is possible to capture and release ammonia efficiently by pressure or temperature swing adsorption techniques using ITQ-29 or FAU zeolites. About 80% of the adsorbed ammonia could be released with small variations of the working conditions. The adsorption and desorption of ammonia in these two zeolites imply great changes in the energy involved in the process. This released energy can be utilized in energy-related applications, such as heat transfer processes. These results together with the relatively high capacity, stability, and commercial availability make these zeolites excellent materials for applications related to the adsorption of ammonia reducing the cost of the actual process. These findings can be extended to other similar systems containing large cavities.

AUTHOR INFORMATION

Corresponding Author

* E-mail: jmviolun@upo.es

* E-mail: scalero@upo.es

Notes

The Authors declare no competing financial interest

ACKNOWLEDGMENT

The research leading to these results has received funding from the Spanish Ministerio de Economía y Competitividad (CTQ2016-80206-P) and Ministerio de Ciencia, Innovación y Universidades (CTQ2017-92173-EXP). We thank C3UPO for the HPC support. JMVl thanks the financial support of the ERC project ZEOSEP (Ref. 779792).

REFERENCES

- 1 E. Cussler, A. McCormick, M. Reese and M. Malmali, Ammonia Synthesis at Low Pressure, *J. Vis. Exp.*, 2017, 1–10.
- 2 N. A. Khan, Z. Hasan and S. H. Jhung, Adsorptive removal of hazardous materials using metal-organic frameworks (MOFs): A review, *J. Hazard. Mater.*, 2013, **244–245**, 444–456.
- 3 C. Petit and T. J. Bandoz, Enhanced adsorption of ammonia on metal-organic framework/graphite oxide composites: Analysis of surface interactions, *Adv. Funct. Mater.*, 2010, **20**, 111–118.
- 4 E. Blázquez, T. Bezerra, J. Lafuente and D. Gabriel, Performance, limitations and microbial diversity of a biotrickling filter for the treatment of high loads of ammonia, *Chem. Eng. J.*, 2017, **311**, 91–99.
- 5 S. Bashkova and T. J. Bandoz, Effect of surface chemical and structural heterogeneity of copper-based MOF/graphite oxide composites on the adsorption of ammonia, *J. Colloid Interface Sci.*, 2014, **417**, 109–114.
- 6 X. Zhang, E. A. Davidson, D. L. Mauzerall, T. D. Searchinger, P. Dumas and Y. Shen, Managing nitrogen for sustainable development, *Nature*, 2015, **528**, 51–59.
- 7 A. F. Bouwman and K. W. Van Der Hoek, Scenarios of animal waste production and fertilizer use and associated ammonia emission for the developing countries, *Atmos. Environ.*, 1997, **31**, 4095–4102.
- 8 R. Sheng, D. Meng, M. Wu, H. Di, H. Qin and W. Wei, Effect of agricultural land use change on community composition of bacteria and ammonia oxidizers, *J. Soils Sediments*, 2013, **13**, 1246–1256.
- 9 M. Altinbas, I. Ozturk and A. F. Aydin, Ammonia recovery from high strength agro industry effluents, *Water Sci. Technol.*, 2002, **45**, 189–196.
- 10 B. Timmer, W. Olthuis and A. Van Den Berg, Ammonia sensors and their applications - A review, *Sensors Actuators, B Chem.*, 2005, **107**, 666–677.
- 11 K. Vikrant, V. Kumar, K. H. Kim and D. Kukkar, Metal-organic frameworks (MOFs): Potential and challenges for capture and abatement of ammonia, *J. Mater. Chem. A*, 2017, **5**, 22877–22896.
- 12 R. E. Critoph and Y. Zhong, Review of trends in solid sorption refrigeration and heat pumping technology, *Proc. Inst. Mech. Eng. Part E J. Process Mech. Eng.*, 2005, **219**, 285–300.
- 13 R. Dunn, K. Lovegrove and G. Burgess, A review of ammonia-based thermochemical energy storage for concentrating solar power BT - SPECIAL ISSUE: The Intermittency Challenge: Massive Energy Storage in a Sustainable Future, *Proc. IEEE*, 2012, **100**, 391–400.
- 14 S. Vasta, V. Brancato, D. La Rosa, V. Palomba, G. Restuccia, A. Sapienza and A. Frazzica, Adsorption Heat Storage: State-of-the-Art and Future Perspectives, *Nanomaterials*, 2018, **8**, 522.
- 15 M. F. de Lange, K. J. F. M. Verouden, T. J. H. Vlugt, J. Gascon and F. Kapteijn, Adsorption-Driven Heat Pumps: The Potential of Metal–Organic Frameworks, *Chem. Rev.*, 2015, **115**, 12205–12250.
- 16 H. G. W. Godfrey, I. da Silva, L. Briggs, J. H. Carter, C. G. Morris, M. Savage, T. L. Easun, P. Manuel, C. A. Murray, C. C. Tang, M. D. Frogley, G. Cinque, S. Yang and M.

- Schröder, Ammonia Storage by Reversible Host–Guest Site Exchange in a Robust Metal–Organic Framework, *Angew. Chemie - Int. Ed.*, 2018, **57**, 14778–14781.
- 17 M. Darestani, V. Haigh, S. J. Couperthwaite, G. J. Millar and L. D. Nghiem, Hollow fibre membrane contactors for ammonia recovery: Current status and future developments, *J. Environ. Chem. Eng.*, 2017, **5**, 1349–1359.
 - 18 J. B. DeCoste, M. S. Denny, G. W. Peterson, J. J. Mahle and S. M. Cohen, Enhanced aging properties of HKUST-1 in hydrophobic mixed-matrix membranes for ammonia adsorption, *Chem. Sci.*, 2016, **7**, 2711–2716.
 - 19 A. J. Rieth, Y. Tulchinsky and M. Dincă, High and Reversible Ammonia Uptake in Mesoporous Azolate Metal–Organic Frameworks with Open Mn, Co, and Ni Sites, *J. Am. Chem. Soc.*, 2016, **138**, 9401–9404.
 - 20 A. J. Rieth and M. Dinca, Controlled Gas Uptake in Metal–Organic Frameworks with Record Ammonia Sorption, *J. Am. Chem. Soc.*, 2018, jacs.8b00313.
 - 21 W. Schirmer, H. Stach, K. Fiedler, W. Rudzinski and J. Jagiello, Adsorption of ammonia in zeolites and SiO₂-molecular sieves. The distribution of adsorption energy in Na-X and NaH-Y zeolites, *Zeolites*, 1983, **3**, 199–204.
 - 22 C. Y. Liu and K. I. Aika, Ammonia Adsorption on Ion Exchanged Y-zeolites as Ammonia Storage Material, *J. Japan Pet. Inst.*, 2003, **46**, 301–307.
 - 23 F. Mazloomi and M. Jalali, Ammonium removal from aqueous solutions by natural Iranian zeolite in the presence of organic acids, cations and anions, *J. Environ. Chem. Eng.*, 2016, **4**, 240–249.
 - 24 R. Xue, A. Donovan, H. Zhang, Y. Ma, C. Adams, J. Yang, B. Hua, E. Inniss, T. Eichholz and H. Shi, Simultaneous removal of ammonia and N-nitrosamine precursors from high ammonia water by zeolite and powdered activated carbon, *J. Environ. Sci. (China)*, 2018, **64**, 82–91.
 - 25 Y. HUANG, C. SONG, L. LI and Y. ZHOU, The Mechanism and Performance of Zeolites for Ammonia Removal in the Zeolite Packed Electrolysis Reactor, *Electrochemistry*, 2014, **82**, 557–560.
 - 26 K. Tsutsumi and K. Nishimiya, Differential molar heats of adsorption of ammonia on silicious mordenites at high temperature, 1989, **143**, 299–309.
 - 27 J. H. E. P. I. T. Jarkko Helminen, Comparison of sorbents and isotherm models for NH₃-gas separation by adsorption, *AIChE J.*, 2000, **46**, 1541–1555.
 - 28 J. Helminen, J. Helenius, E. Paatero and I. Turunen, Adsorption Equilibria of Ammonia Gas on Inorganic and Organic Sorbents at 298.15 K, *J. Chem. Eng. Data*, 2001, **46**, 391–399.
 - 29 E. Jaramillo and M. Chandross, Adsorption of Small Molecules in LTA Zeolites. 1. NH₃, CO₂, and H₂O in Zeolite 4A, *J. Phys. Chem. B*, 2004, **108**, 20155–9.
 - 30 D. Frenkel and B. Smit, *Understanding Molecular Simulations: From Algorithms to Applications*, C. Academic Press, San Diego, CA, second edi., 2002.
 - 31 D. Dubbeldam, S. Calero, D. E. Ellis and R. Q. Snurr, RASPA: Molecular Simulation Software for Adsorption and Diffusion in Flexible Nanoporous Materials, *Mol. Simul.*, 2016, **42**, 81–101.
 - 32 D. Dubbeldam, A. Torres-Knoop and K. S. Walton, On the inner workings of Monte Carlo codes, *Mol. Simul.*, 2013, **39**, 1253–1292.

- 33 I. Matito-Martos, A. Martin-Calvo, J. J. Gutiérrez-Sevillano, M. Haranczyk, M. Doblare, J. B. Parra, C. O. Ania and S. Calero, Zeolite screening for the separation of gas mixtures containing SO₂, CO₂ and CO., *Phys. Chem. Chem. Phys.*, 2014, **16**, 19884–19893.
- 34 E. Garcia-Perez, J. B. Parra, C. O. Ania, A. Garcia-Sanchez, J. M. Van Baten, R. Krishna, D. Dubbeldam and S. Calero, A computational study of CO₂, N₂, and CH₄ adsorption in zeolites, *Adsorpt. Int. Adsorpt. Soc.*, 2007, **13**, 469–476.
- 35 L. Zhang and J. I. Siepmann, Development of the trappe force field for ammonia, *Collect. Czechoslov. Chem. Commun.*, 2010, **75**, 577–591.
- 36 M. P. Allen and D. J. Tildesley, *Computer Simulation of Liquids*, Oxford Clarendon Press, Oxford, Second Edi., 2017.
- 37 National Institute of Standards and Technology, <http://www.nist.gov/index.html>.
- 38 A. Garcia-Sanchez, C. O. Ania, J. B. Parra, D. Dubbeldam, T. J. H. Vlugt, R. Krishna and S. Calero, Transferable Force Field for Carbon Dioxide Adsorption in Zeolites, *J. Phys. Chem. C*, 2009, **113**, 8814–8820.
- 39 W. L. Jorgensen and J. Gao, Monte Carlo Simulations of the Hydration of Ammonium and Carboxylate Ions, *J. Phys. Chem.*, 1986, **90**, 2174–2182.
- 40 T. J. H. Vlugt and M. Schenk, Influence of framework flexibility on the adsorption properties of hydrocarbons in the zeolite silicalite, *J. Phys. Chem. B*, 2002, **106**, 12757–12763.
- 41 J. Baker, An algorithm for the location of transition states, *J. Comput. Chem.*, 1986, **7**, 385–395.
- 42 M. J. Sanders, M. Leslie and C. R. A. Catlow, Interatomic Potentials for SiO₂, *J. CHEM. SOC., CHEM. COMMUN.*, 1984, **0**, 1271–1273.
- 43 R. A. Jackson and C. R. A. Catlow, Computer Simulation Studies of Zeolite Structure, *Mol. Simul.*, 1998, **1**, 207–224.
- 44 S. R. G. Balestra, S. Hamad, A. R. Ruiz-Salvador, V. Domínguez-García, P. J. Merklings, D. Dubbeldam and S. Calero, Understanding Nanopore Window Distortions in the Reversible Molecular Valve Zeolite RHO, *Chem. Mater.*, 2015, **27**, 5657–5667.
- 45 J. G. Min, A. Luna-Triguero, Y. Byun, S. R. G. Balestra, J. M. Vicent-Luna, S. Calero, S. B. Hong and M. A. Camblor, Stepped Propane Adsorption in Pure-Silica ITW Zeolite, *Langmuir*, 2018, **34**, 4774–4779.
- 46 B. Widom, Some Topics in the Theory of Fluids, *J. Chem. Phys.*, 1963, **39**, 2808.
- 47 L. Sarkisov and A. Harrison, Computational structure characterisation tools in application to ordered and disordered porous materials, *Mol. Simul.*, 2011, **37**, 1248–1257.
- 48 L. D. Gelb and K. E. Gubbins, Pore Size Distributions in Porous Glasses: A Computer Simulation Study, *Langmuir*, 2002, **15**, 305–308.
- 49 E. . Garcia-Perez, J. B. . Parra, C. O. . Ania, D. . Dubbeldam, T. J. H. . Vlugt, J. M. . Castillo, P. J. . Merklings and S. Calero, Unraveling argon adsorption processes in MFI-type zeolite, *J. Phys. Chem. C*, 2008, **112**, 9976–9979.
- 50 C. A. Fyfe, H. Strobl, G. T. Kokotailo, G. J. Kennedy and G. E. Barlow, Ultra-high-resolution ²⁹Si solid-state MAS NMR investigation of sorbate and temperature-induced changes in the lattice structure of zeolite ZSM-5, *J. Am. Chem. Soc.*, 1988, **110**, 3373–3380.

- 51 E. L. Wu, S. L. Lawton, D. H. Olson, A. C. Rohrman and G. T. Kokotallo, ZSM-5-type materials. Factors affecting crystal symmetry, *J. Phys. Chem.*, 1979, **83**, 2777–2781.
- 52 H. van Koningsveld, H. van Bekkum and J. C. Jansen, On the location and disorder of the tetrapropylammonium (tpa) ion in zeolite ZSM-5 with improved framework accuracy, *Acta Crystallogr. Sect. B-Structural Sci.*, 1987, **43**, 127–132.
- 53 H. van Koningsveld, J. C. Jansen and H. van Bekkum, The monoclinic framework structure of zeolite H-ZSM-5. Comparison with the orthorhombic framework of as-synthesized ZSM-5, *Zeolites*, 1990, **10**, 235–242.
- 54 A. Corma, F. Rey, J. Rius, M. J. Sabater and S. Valencia, Supramolecular self-assembled molecules as organic directing agent for synthesis of zeolites, *Nature*, 2004, **431**, 287–290.
- 55 J. A. Hriljac, M. M. Eddy, A. K. Cheetham, J. A. Donohue and G. J. Ray, Powder neutron-diffraction and ²⁹Si NMR studies of siliceous zeolite-Y, *J. Solid State Chem.*, 1993, **106**, 66–72.
- 56 A. Martín-Calvo, J. J. Gutiérrez-Sevillano, J. B. Parra, C. O. Ania, S. Calero, J. J. Gutiérrez-Sevillano, J. B. Parra, C. O. Ania and S. Calero, Transferable force fields for adsorption of small gases in zeolites, *Phys. Chem. Chem. Phys.*, 2015, **17**, 24048–24055.
- 57 R. Krishna, J. M. van Baten, E. Garcia-Perez and S. Calero, Incorporating the loading dependence of the Maxwell-Stefan diffusivity in the modeling of CH₄ and CO₂ permeation across zeolite membranes, *Ind. Eng. Chem. Res.*, 2007, **46**, 2974–2986.
- 58 K. Zhang, R. P. Lively, J. D. Noel, M. E. Dose, B. A. McCool, R. R. Chance and W. J. Koros, Adsorption of water and ethanol in MFI-type zeolites, *Langmuir*, 2012, **28**, 8664–8673.
- 59 S. Yi, Y. Su and Y. Wan, Preparation and characterization of vinyltriethoxysilane (VTES) modified silicalite-1/PDMS hybrid pervaporation membrane and its application in ethanol separation from dilute aqueous solution, *J. Memb. Sci.*, 2010, **360**, 341–351.
- 60 X. Yang, L. Huang, J. Li, X. Tang and X. Luo, Fabrication of SiO₂@silicalite-1 and its use as a catalyst support, *RSC Adv.*, 2017, **7**, 12224–12230.
- 61 R. Grau-Crespo, E. Acuay and A. Rabdel Ruiz-Salvador, A free energy minimisation study of the monoclinic-orthorhombic transition in MFI zeolite, *Chem. Commun.*, 2002, **8**, 2544–2545.
- 62 M. Ardit, A. Martucci and G. Cruciani, Monoclinic orthorhombic phase transition in ZSM 5 zeolite: Spontaneous strain variation and thermodynamic properties, *J. Phys. Chem. C*, 2015, **119**, 7351–7359.
- 63 A. Lopez, M. Souldard and J. L. Guth, Temperature-induced monoclinic/ orthorhombic transition in germanium MFI-type zeolites, *Zeolites*, 1990, **10**, 134–136.
- 64 ZEOLYST, <https://www.zeolyst.com/>, (accessed 24 April 2019).
- 65 M. A. Ricci, M. Nardone, F. P. Ricci, C. Andreani and A. K. Soper, Microscopic structure of low temperature liquid ammonia: A neutron diffraction experiment, *J. Chem. Phys.*, 1995, **102**, 7650–7655.
- 66 A. D. Boese, A. Chandra, J. M. L. Martin and D. Marx, From ab initio quantum chemistry to molecular dynamics: The delicate case of hydrogen bonding in ammonia, *J. Chem. Phys.*, 2003, **119**, 5965–5980.
- 67 L. L. He, S. Y. Zhang, T. T. Sun, C. L. Zhao, C. Zhang, Z. Z. Yang and D. X. Zhao, Study on properties of liquid ammonia via molecular dynamics simulation based on

ABEEM $\sigma\pi$ polarisable force field, *Mol. Simul.*, 2017, **43**, 1099–1106.

- 68 D. Chakraborty and A. Chandra, Hydrogen bonded structure and dynamics of liquid-vapor interface of water-ammonia mixture: An ab initio molecular dynamics study, *J. Chem. Phys.*, 2011, **135**, 1–11.